AD NUMBER

AD479435

LIMITATION CHANGES

TO:

Approved for public release; distribution is unlimited.

FROM:

**Distribution authorized to U.S. Gov't. agencies and their contractors;
Administrative/Operational Use; SEP 1950. Other requests shall be referred to Army Ballistic Research Laboratory, Aberdeen Proving Ground, MD 21010.**

AUTHORITY

bal d/a ltr 22 apr 1981

BALLISTIC RESEARCH LABORATORIES

REPORT NO. 731

Optimum Source Size for the Mach-Zehnder Interferometer

F. D. BENNETT

ABERDEEN PROVING GROUND, MARYLAND

B A L L I S T I C R E S E A R C H L A B O R A T O R I E S

REPORT NO. 731

September 1950

OPTIMUM SOURCE SIZE FOR THE MACH-ZEHNDER INTERFEROMETER

F. D. Bennett

Project No. TB3-0108C of the Research and
Development Division, Ordnance Corps

A B E R D E E N P R O V I N G G R O U N D, M A R Y L A N D

TABLE OF CONTENTS

BALLISTIC RESEARCH LABORATORIES REPORT NO. 731

Bennett/emj
Aberdeen Proving Ground, Md.
5 September 1950

OPTIMUM SOURCE SIZE FOR THE MACH-ZEHNDER INTERFEROMETER

ABSTRACT

A vector analytic treatment is given of the formation of undisturbed fringes by an ideal Mach-Zehnder interferometer with an extended source. The path difference of two interfering rays at an arbitrary point in the field is found to depend in a simple way upon the source point from which the rays originate, the field point examined, and a dyadic which is a function of the unit normals to the last mirror and divider plate of the interferometer. The fringe clarity condition that all pairs of interfering rays reaching the field point have path differences within a specified range is developed in the form of an inequality. Analysis of this fundamental inequality shows that all admissible area sources must be areas enclosed between two conics in the source plane. For fringes perpendicular to the plane of centers of the interferometer elements, the optimum source is a circle with radius inversely proportional to the square root of the number of clear fringes desired. This result holds for all interferometers of parellelogram planform. For fringes parallel to the plane of centers, each interferometer orientation presents a special case. The optimum source area is obtained for two of these, viz., the 45° and 30° interferometers.

1. INTRODUCTION

In recent years much attention has been devoted to the Mach-Zehnder interferometer as an instrument suitable for the exploration of supersonic flows. A paper by J. Winkler[1] reports the application of this instrument to the study of an axially symmetric supersonic jet of air, and, in describing the theory of the interferometer, the author remarks (p. 309), "The complete theory of the formation of inteference fringes from a large, extended source by the Mach interferometer has not been given so far." At about the same time, a Naval Ordnance Laboratory report by Ernst Winkler[2] appeared in which a thorough study of the Mach-Zehnder interferometer was made, employing synthetic geometrical methods and many geometrical figures and diagrams. While E. Winkler's work gives a partial answer to the question of optimum source size, his synthetic technique is complicated and hard to follow requiring considerable effort on the part of the reader in visualizing the conditions described.

In this paper, a vector analytic treatment of the ideal Mach-Zehnder interferometer will be given. The problem of optimum source size and shape will be seen to be completely solvable for a large class of interferometers; furthermore, the general results will be obtained in concise, mnemonic form.

2. GENERAL VECTOR EQUATIONS

Several results from vector analytic geometry will be collected here for convenience.

In three-space, the equation of a plane with unit normal $\underline{\bar{n}}$ passing through point $\underline{\bar{x}_o}$ is

$$(\bar{x} - \bar{x}_o) \cdot \bar{n} = 0. \qquad (1)$$

---

[1] J. Winkler, "The Mach Interferometer Applied to Studying an Axially Symmetric Supersonic Air Jet," Rev. Sci. Inst., 19, 307, (1948).

[2] E. H. Winkler, "Analytical Studies of the Mach-Zehnder Interferometer," N. O. L. Report No. 1077 (5 December 1947).

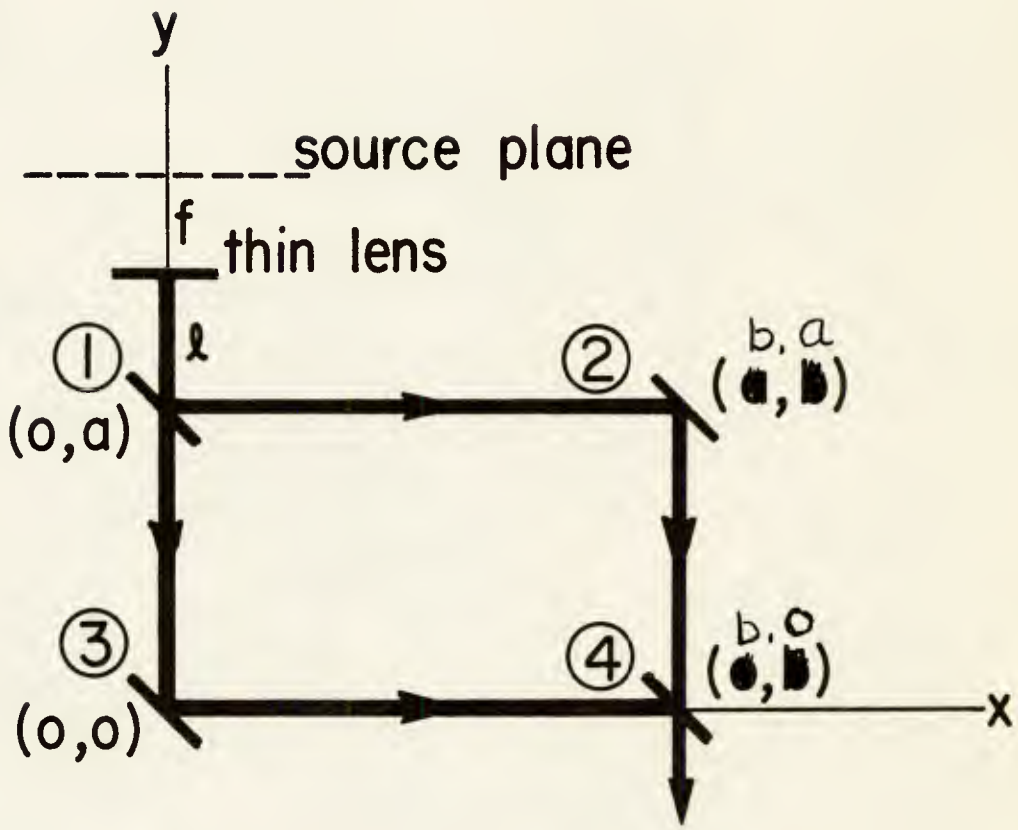

FIG. 1 — STANDARD INTERFEROMETER CONFIGURATION.

ARMY---OS---ABERDEEN PROVING GROUND, MD---281

The equation for a line passing through point $\bar{x}_p$ in the direction of the unit vector $\bar{r}$ is

$$\bar{x} - \bar{x}_p = s\bar{r} \tag{2}$$

where s is the magnitude of the distance from $\bar{x}_p$ to $\bar{x}$. The perpendicular distance from the point $\bar{x}_p$ to the plane (1) is found by replacing $\bar{r}$ in (2) by the normal $\bar{n}$ and requiring that $\bar{x}$ be the point of intersection of the line with the plane; thus

$$s_\perp = (\bar{x}_o - \bar{x}_p) \cdot \bar{n} \quad . \tag{3}$$

To treat the reflection of light from a plane mirror, we need to obtain the unit vector of the outgoing ray $\bar{r}_j$ in terms of the unit vector of the incoming ray $\bar{r}_{j-1}$ and the normal to the plane $\bar{n}_j$. The laws of reflection are expressed by the equations

$$(\bar{r}_j \cdot \bar{n}_j) = -(\bar{r}_{j-1} \cdot \bar{n}_j)$$

and

$$\bar{r}_j = a\bar{r}_{j-1} + b\bar{n}_j \ .$$

These with the requirement that $\bar{r}_j^2 = 1$ yield

$$\bar{r}_j = \bar{r}_{j-1} - 2(\bar{r}_{j-1} \cdot \bar{n}_j)\,\bar{n}_j \tag{4}$$

By exactly similar reasoning, one could express the normal $\bar{n}_j$ in terms of $\bar{r}_j$ and $\bar{r}_{j-1}$ assuming these to be known.

3. SPECIFICATION OF THE INTERFEROMETER

We shall consider only interferometers made of ideal elements. The collimating and camera lenses are assumed to be perfect thin lenses. The dividing plates and mirrors are assumed to be perfectly plane and of zero thickness, producing no changes other than beam division and/or change of direction of the incident light.

To specify a standard interferometer configuration, consider a plane rectangle of sides a, b in the x, y plane with its lower left-hand corner at the origin and sides parallel to the x and y directions. The elements of the interferometer are located as in Figure 1 with their centers on the corners of the rectangle and lie in vertical planes whose traces have slope -1. Thus, we have a 45° interferometer in standard position with element (1), the first divider plate, at (o, a); element (2), a reflecting mirror, at (b, a); element (3), reflecting mirror, at (o, o); and element (4), the second divider plate, at (b, o). The unit normals $\bar{n}_1$ and $\bar{n}_3$ corresponding to

elements (1) and (3) lie in the x, y plane at 45° with the $\underline{x}$ axis and pointing into the first quadrant; while the unit normals $\underline{n}_2$, $\underline{n}_4$ are anti-parallel with $\underline{n}_1$, $\underline{n}_3$. Parallel light entering the interferometer from the collimating lens at $(o, a + \ell)$ proceeds in the negative $\underline{y}$ direction to (1) where it is divided into two beams which pass through the interferometer along opposite sides of the rectangle to be recombined at (4), there to exit again in the negative direction.

If the source illuminating the interferometer consists of a single point on the $\underline{y}$ axis at $(o, a + \ell + f)$, where f is the focal length of the lens, the collimator will form a single parallel beam which may be characterized by the unit vector $\underline{r}_c$ located at the center of the lens and pointing in the negative $\underline{y}$ direction. This type of source is that commonly employed in discussing the elementary theory of the interferometer. The $\underline{r}_c$ unit vector has the property of lying at the center of the beam and pointing along its axis; thus, it is capable of representing each ray in the beam; furthermore, planes with $\underline{r}_c$ as normal intersect the beam in surfaces of constant phase.

If an extended area source in the focal plane of the lens be considered, it is clear that the lens produces a parallel beam corresponding to each point on the source and characterized by the unit vector $\underline{r}$, with origin at the center of the lens, directed along the line joining source point with lens center. A source of arbitrary shape is seen to give rise to a bundle of unit vectors whose tips lie on the unit sphere with origin at the center of the lens. In considering the formation of fringes by the interferometer, it is helpful to regard this bundle of unit vectors as if it were a luminous object replacing the lens and source altogether.

The effect of the interferometer is to split each beam arising from a single source-point into two coherent beams of parallel light, allowing them to traverse equal paths before recombination at plate (4).

In terms of the characteristic unit vectors $\underline{r}$, the interferometer produces two, virtual bundles of unit vectors at a distance $L = a + b + \ell$ above plate (4). With (4) at 45°, these virtual images exactly overlap and no fringes are formed. If (4) is rotated through a small angle $\epsilon/2$ leaving its center fixed, one of the virtual images is rotated about the same center on a radius L, through the angle ϵ. In general, the bundle of vectors is also rotated like a rigid body about line L as the axis of rotation.

Since the reflection from (2) fixes the position of the unrotated bundle of unit vectors, the representative vector denoted by $\underline{r}$ at the lens will become $\underline{r}_2$ at mirror (2) in conformity with the notation of

equation (4). As the reflection from ④ fixes the position of the rotated bundle, its representative vector will become $\bar{r}_4$. The result then is two diverging pencils of parallel beams so oriented that the central beams of each, characterized by virtual $\bar{r}_{2c}$ and its displaced image $\bar{r}_{4c}$ converge toward the center of plate ④.

While in practice fringes are rarely obtained by adjustment of plate ④ alone, for the purposes of the analysis it is most convenient to regard all other elements as fixed and rotate ④. As will be seen later, the analysis of this case can be applied without modification to a large class of adjustments involving three elements of the interferometer.

4. DERIVATION OF THE PATH DIFFERENCE d

The central problem before us is to examine at an arbitrary field point $\bar{x}_p$ (with origin now determined at the center of plate ④), the phase of any pair of interfering rays reaching the point. This we may do by recalling that the first divider plate produces two and only two beams from each point on the source. Any pair of rays from these two beams may combine to cause interference. Rays selected from beams belonging to different source points will not interfere because of lack of coherence. Since we have already seen that the unit vector $\bar{r}$ at the lens splits into $\bar{r}_2$ and $\bar{r}_4$, we have in these vectors the identification of corresponding pairs of coherent beams. Rays proceed parallel to these unit vectors in the respective beams; we have only to determine the perpendicular distance from point $\bar{x}_p$ to the initial planes of equal phase, viz., the planes passing through the origins of the virtual bundles of vectors. The difference of these distances is the path difference d which governs the phase of the interference of the two rays.

To find these origins, we utilize the fact that the virtual bundles of vectors appear at distance -L from the center of ④ in the $\bar{r}_{2c}$ and $\bar{r}_{4c}$ directions,

thus
$$\bar{x}_2 = -L\bar{r}_{2c}$$
and
$$\bar{x}_4 = -L\bar{r}_{4c} \qquad (5)$$

from equation (2).

The perpendicular distance from $\bar{x}_p$ to the plane passing through $\bar{x}_2$ with normal $\bar{r}_2$ is by (3)

$$s_2 = (\bar{x}_2 - \bar{x}_p) \cdot \bar{r}_2 \quad ;$$

similarly for the plane passing through $\bar{x}_4$ with normal $\bar{r}_4$

$$s_4 = (\bar{x}_4 - \bar{x}_p) \cdot \bar{r}_4 \quad .$$

The path difference

$$\begin{aligned} d = s_4 - s_2 &= (\bar{x}_4 - \bar{x}_p) \cdot \bar{r}_4 - (\bar{x}_2 - \bar{x}_p) \cdot \bar{r}_2 \\ &= L\,(\bar{r}_{2c} \cdot \bar{r}_2 - \bar{r}_{4c} \cdot \bar{r}_4) + (\bar{r}_2 - \bar{r}_4) \cdot \bar{x}_p \end{aligned} \tag{6}$$

using equations (5).

Now from (4) we find by substitution

$$\bar{r}_j \cdot \bar{r}_{jc} = \bar{r}_{j-1} \cdot \bar{r}_{j-1c} \tag{7}$$

which expresses the invariance of angle between two rays under plane reflection. Using (7) to trace back through the elements of the interferometer, we establish that

$$\bar{r}_2 \cdot \bar{r}_{2c} = \bar{r}_4 \cdot \bar{r}_{4c} = \bar{r} \cdot \bar{r}_c \quad ; \tag{8}$$

thus (6) reduces to

$$d = (\bar{r}_2 - \bar{r}_4) \cdot \bar{x}_p \quad . \tag{9}$$

We see that the path difference expression is independent of any lengths characteristic of the inteferometer so long as the origins of the virtual unit vectors lie the same distance, $-L$, behind the center of ④ in the $\bar{r}_{2c}$ and $\bar{r}_{4c}$ directions.

An immediate broadening in two directions of the class of inteferometers covered by this analysis is now possible. In the first place, the rectangle may be sheared in the y direction into a parallelogram with vertical sides. The central rays formed by splitting $\bar{r}_c$ at ① traverse the sides of the parallelogram providing that the normals of the interferometer elements are adjusted to bisect the acute angles into which they point, retaining $\bar{n}_1$, $\bar{n}_3$ parallel as before and anti-parallel to $\bar{n}_2$, $\bar{n}_4$ prior to rotation of $\bar{n}_4$ to produce fringes. Such a sheared interferometer will be denoted by the angle between $\bar{n}_1$ and the vertical, e.g., a 30° interferometer is one in which the traces of the plates in standard position are inclined at 30° to the negative x direction; $\bar{n}_1$, $\bar{n}_3$ thus make 30° with the vertical.

Secondly, the origin may be moved from the center of ④ to any line y = const. between ② and ④ (or exterior to this segment for that matter) still preserving the essential conditions which

lead to equation (9). One way of doing this is to rotate $\bar{n}_1$ toward the vertical and translate (2) vertically so that the central ray from (1) is still incident on the center of (2) but rotating its normal so that $\bar{r}_{2c}$ is no longer vertical, then rotation of (4) in the appropriate direction will give an intersection of $\bar{r}_{2c}$ and $\bar{r}_{4c}$ which defines the new origin.

It is easily shown that given θ and ϕ the angles through which $\bar{n}_2$ and $\bar{n}_4$ are to be rotated and y_o the vertical distance to the new origin measured from the center of (4), there always exists a real solution to the problem of specifying α the angle of rotation of $\bar{n}_1$ (and the vertical translation of (2) which depends upon α) in such a way that equations (5) are preserved with an appropriate value of the parameter L.

5. ANALYSIS OF THE PATH DIFFERENCE FORMULA

To develop equation (9) further, let us trace the representative (beam) vector $\bar{r}$ through the interferometer using (4). Since $\bar{n}_1 = -\bar{n}_2$ we have

$$\bar{r}_2 = \bar{r} \tag{10}$$

$$\bar{r}_3 = \bar{r} - 2(\bar{r} \cdot \bar{n}_3)\,\bar{n}_3 \tag{11}$$

and

$$\bar{r}_4 = \bar{r}_3 - 2(\bar{r}_3 \cdot \bar{n}_4)\,\bar{n}_4 \,. \tag{12}$$

Substituting these equations into (9) gives

$$d = 2\bar{r} \cdot D \cdot \bar{x}_p \tag{13}$$

where

$$D = \left[\bar{n}_3\bar{n}_3 - 2\bar{n}_3\,(\bar{n}_3 \cdot \bar{n}_4)\,\bar{n}_4 + \bar{n}_4\bar{n}_4\right]. \tag{14}$$

D is a dyad or matrix and in (13) is operated on from the left by dotting in $\bar{r}$, from the right by dotting in $\bar{x}_p$. This remarkably simple result allows us to express the path difference of interfering rays from source point $\bar{r}$ at any field point $\bar{x}_p$ providing we know the unit normals $\bar{n}_3$, $\bar{n}_4$ of the interferometer.

It is immediately clear from the form of D that there is no contribution to d from any component of $\bar{x}_p$ in the direction $\bar{n}_4 \times \bar{n}_3$, i.e., d is constant along lines in the $\bar{n}_4 \times \bar{n}_3$ direction. This direction is therefore the direction of clear fringes formed by the interferometer. Vertical fringes* are formed when $\bar{n}_3$, $\bar{n}_4$ remain in

---

* Henceforth the adjective "vertical" designates fringes perpendicular to the plane of centers of the interferometer elements while "horizontal" designates fringes parallel to this plane.

the plane of centers while horizontal fringes occur when $\bar{n}_4$ is rotated in a plane containing $\bar{n}_3$ and perpendicular to the plane of centers.

The character of the fringes may be seen from the following. Fringes are curves of intersection between the plane of observation (photographic plate) and surfaces of constant path difference d. For d = const. and a given $\bar{r}$ (source point) (13) is the equation of the family of parallel planes with normal $\bar{r} \cdot D$. As $\bar{r} \cdot D$ is a linear function of $\bar{n}_3$ and $\bar{n}_4$, the planes themselves are perpendicular to the plane of $\bar{n}_3$, $\bar{n}_4$ and thus parallel to the $\bar{n}_4 \times \bar{n}_3$ direction regardless of $\bar{r}$. For point source $\bar{r} = \bar{r}_c$ the planes of constant path difference are very closely parallel to $\bar{r}_c$ and the fringes will be parallel straight lines (not necessarily parallel to $\bar{n}_4 \times \bar{n}_3$). For a source point off the axis the corresponding family of planes does not intersect the plate along the same straight lines as before. The separation between the fringes for $\bar{r}_c$ and $\bar{r}$ is zero at the origin and increases both linearly with x and as a function of the angle between $\bar{r} \cdot D$ and $\bar{r}_c \cdot D$; hence with an extended source the composite fringes while unchanging in the $\bar{n}_4 \times \bar{n}_3$ direction become progressively fuzzier with distance from the origin.

If the plane of observation contains $\bar{n}_4 \times \bar{n}_3$ the fringes are of course parallel to this direction. Rotation of the plane about $\bar{n}_4 \times \bar{n}_3$ causes the fringe spacing to pass through a relative minimum, as will be seen later from the fringe width equation (22). It is reasonable to suppose that the sharpest fringes will occur for the narrowest fringe width, i.e., at the relative minimum; since otherwise the fuzziness caused by an extended source is projected onto a wider area and contrast of the fringes is reduced.

D may be further modified to advantage if we set

$$\bar{n}_4 = a\bar{n}_3 + b\bar{t} \tag{15}$$

where $\bar{t}$ is a unit vector in the $\bar{n}_3 \times (\bar{n}_4 \times \bar{n}_3)$ direction. (Note that $\bar{n}_3$, $\bar{n}_4 \times \bar{n}_3$, $\bar{t}$ form a right-handed triad).

Since $\bar{n}_3 \cdot \bar{n}_4 = -\cos \epsilon/2$ and $\bar{n}_4^2 = 1$, we find

$$\bar{n}_4 = -\cos \epsilon/2\, \bar{n}_3 + \sin \epsilon/2\, \bar{t} \tag{16}$$

and

$$D = \sin \epsilon/2 \left[\sin \epsilon/2\, \bar{n}_3\bar{n}_3 + \cos \epsilon/2\, (\bar{n}_3\bar{t} - \bar{t}\bar{n}_3) + \sin \epsilon/2\, \bar{t}\bar{t} \right] \tag{17}$$

where $\epsilon/2$ is the angle of rotation of $\bar{n}_4$ to produce fringes.

Since no component of $\bar{x}_p$ in the $\bar{n}_4 \times \bar{n}_3$ direction has any effect on d there is no loss in assuming henceforth that $\bar{x}_p$ lies entirely in the plane of $\bar{n}_3$, $\bar{t}$ perpendicular to $\bar{n}_4 \times \bar{n}_3$. Let

$$\bar{x}_p = \bar{x} = x\,(\bar{n}_3 \sin \psi + \bar{t} \cos \psi). \tag{18}$$

Substituting (18) and (17) into (13) we obtain

$$d = 2\,x \sin \epsilon/2\; \bar{r} \cdot \bar{p} \tag{19}$$

where

$$\bar{p} = \bar{n}_3 \cos (\psi - \epsilon/2) - \bar{t} \sin (\psi - \epsilon/2). \tag{20}$$

$\bar{x}$ is the vector to the field point under examination in the plane normal to $\bar{n}_4 \times \bar{n}_3$. $\bar{p}$ is a unit vector in the same plane but approximately perpendicular to $\bar{x}$, as may be seen from

$$\bar{p} \cdot \bar{x} = x \sin \epsilon/2 \doteq 0. \tag{21}$$

Now $\bar{r} \cdot \bar{p}$ is the cosine of the angle ϕ between $\bar{r}$ and $\bar{p}$ and depends upon the source point represented by $\bar{r}$ and upon the vector $\bar{p}$ which is very closely normal to the direction of investigation in the field of fringes, i.e., normal to the photographic plate. Using (19), if

$$\left| d_2 - d_1 \right| = \lambda = 2 \sin \epsilon/2 \left| (\bar{r} \cdot \bar{p})\,(x_2 - x_1) \right|$$

then the fringe width is

$$w = \left| x_2 - x_1 \right| = \frac{\lambda}{2 \sin \epsilon/2 \left| (\bar{r} \cdot \bar{p}) \right|}. \tag{22}$$

Some further information regarding the fringe pattern may now be obtained. w takes on its smallest value for a given $\epsilon/2$ when $\left| \bar{r} \cdot \bar{p} \right| = 1$, i.e., $\bar{r}$ and $\bar{p}$ are parallel or anti-parallel. As $\bar{p}$ lies in the plane of $\bar{n}_3$ and $\bar{n}_4$, and $\bar{r}$ will usually lie close to $\bar{r}_c$, the minimum w will be attained only when $\bar{r}_c$ lies in or near the $\bar{n}_3$, $\bar{n}_4$ plane, i.e., perpendicular to $\bar{n}_4 \times \bar{n}_3$. As $\bar{n}_4 \times \bar{n}_3$ lies always in the plane normal to $\bar{n}_3$, it will be perpendicular to $\bar{r}_c$ only when also perpendicular to the plane of centers. This is the condition for vertical fringes. Other fringe orientations produce relative minima larger than that for vertical fringes, e.g., for $\bar{n}_4 \times \bar{n}_3$ horizontal, $\left| \bar{r} \cdot \bar{p} \right| = \cos \Theta$ where Θ is the angle of the interferometer.

For vertical fringes with point source $\bar{r} = \bar{r}_c$ we may have $\left| \bar{r}_c \cdot \bar{p} \right| = 1$ and (22) assumes the familiar standard form

$$w_s = \frac{\lambda}{2 \sin \epsilon/2} \doteq \lambda/\epsilon \ . \qquad (23)$$

The conjecture made earlier in the paragraph that laterally sharpest fringes are associated with minimum fringe width leads to the conclusion that vertical fringes with $\bar{p} \cdot \bar{r}_c = 1$ will be sharpest of all. As $\bar{p}$ is normal to the $\bar{x}$ direction in the photographic plate within $\epsilon/2$, we see that the usual arrangement where vertical fringes are observed on a plate normal to $\bar{r}_c$ is actually very close to the best possible and (23) applies.

6. FUNDAMENTAL INEQUALITY

Equation (22) shows the dependence of fringe width on the position of the source point represented by $\bar{r}$; thus an extended area source will produce a composite fringe system consisting of an infinite set of overlapping fringe systems. All those source points producing patterns with the same fringe width are characterized by the requirement

$$\bar{r} \cdot \bar{p} = \cos \phi = \text{const.} \qquad (24)$$

(24) restricts the vectors $\bar{r}$ to lie on the cone with vertex at the center of the unit sphere and generator making angle ϕ with the unit vector $\bar{p}$. The intersection of this cone with the plane of the source, whose normal is $\bar{r}_c$, gives the source curve which produces the given fringe width. This curve is, of course, a conic section.

In order to obtain a clear fringe system we must require either that the source consist only of points for which d = const. and (24) follows, or we must require that d differ by a small preassigned quantity from the predetermined constant value. The second alternative is less restrictive than the first and will lead to area-type sources which are practically realizable. Selecting d_c as the comparison value, i.e., in effect choosing the path difference for the central source point as the standard, we write

$$\left| d - d_c \right| \leq K \lambda \qquad (25)$$

where K is a suitably small number depending upon the clarity that we require in the fringe system.

We shall call this expression the fundamental inequality of the Mach-Zehnder interferometer. It is a generalization of the form used by E. H. Winkler in derivation of his equation (2). From it

can be deduced the size and shape of an admissible source for any interferometer of the class specified in Section 4 with any desired orientation of fringes.

While d_c has been selected as the comparison value in (25), situations may arise where some advantage may be obtained by excluding the central source point. In such a case, a suitable reference value of d should be chosen and substituted for d_c.

Returning to (19) we see that for $x = 0$ $d = 0$ and we have the central fringe condition for which all source points have zero path difference. Proceeding in + or - x direction the path difference increases linearly as one passes through fringes 0, ± 1, ± 2, ± 3.... A simplification in (19) occurs if we agree to measure x in units of standard fringe width w_s. Using (23), the expression for w_s, (19) becomes

$$d = N \lambda \bar{r} \cdot \bar{p} \tag{26}$$

and (25)

$$\left| \bar{r} \cdot \bar{p} - \bar{r}_c \cdot \bar{p} \right| \leq \frac{K}{N} \tag{27}$$

where we now understand N to be positive. For most practical situations, the actual fringe width differs so little from the standard w_s that the number N gives accurately the number of fringes on either side of center for which the fundamental inequality is satisfied. In using (27), we may specify the number of fringes we desire within a given clarity criterion rather than specifying the size of the field to be investigated.

Inequality (27) is unchanged if we replace $\bar{r}$ and $\bar{r}_c$ by their negatives. The advantages are twofold: 1) $0 \leq \bar{r}_c \cdot \bar{p} \leq 1$, i.e., ϕ_c is an acute angle and representation of $\bar{p}$ and $\bar{r}_c$ on the unit sphere is easier to visualize; 2) $\bar{r}_c$ is now directed along the axis toward the source plane whose equation relative to the center of the sphere is

$$(\bar{x} - f\bar{r}_c) \cdot \bar{r}_c = 0 \ . \tag{28}$$

The fundamental inequality may now be written as

$$\bar{r}_c \cdot \bar{p} - \frac{K}{N} \leq \bar{r} \cdot \bar{p} \leq \bar{r}_c \cdot \bar{p} + \frac{K}{N} \tag{29}$$

or

$$\cos \phi_c - \frac{K}{N} \leq \cos \phi \leq \cos \phi_c + \frac{K}{N} \ . \tag{30}$$

We see that the permissible $\bar{r}$ vectors lie on the unit sphere between the two cones whose generators make angles

$$\phi = \cos^{-1} \left(\cos \phi_c \pm \frac{K}{N} \right) \tag{31}$$

with vector $\bar{p}$. In the plane (28), the permissible source may occupy the area contained between the conics formed by the intersections of the cones with the plane.

The equation of the conic in the source plane is easily found if we employ the orthogonal triad of unit vectors

$$\begin{aligned} \bar{r}_c & \\ \bar{\rho} &= \frac{\bar{p} \times \bar{r}_c}{\sin \phi_c} \\ \bar{\eta} &= \frac{\bar{r}_c \times (\bar{p} \times \bar{r}_c)}{\sin \phi_c} \end{aligned} \tag{32}$$

and construct the vector

$$\bar{R} = f\bar{r}_c + x\,\bar{\eta} + y\bar{\rho} \tag{33}$$

which satisfies the equation of the plane (28). The requirement that $\bar{R}$ be a generator of the cone is

$$\frac{\bar{R} \cdot \bar{p}}{|\bar{R}|} = \cos \phi \quad ; \tag{34}$$

whence using (32) (33) and simplifying we have the standard form

$$\frac{\bar{X}^2}{a^2} + \frac{\bar{Y}^2}{b^2} = 1 \tag{35}$$

with

$$\left.\begin{aligned} \bar{X} &= x - \frac{f \sin \phi_c \cos \phi_c}{\cos^2 \phi - \sin^2 \phi_c} \\ a^2 &= \frac{f^2 \sin^2 \phi \cos^2 \phi}{(\cos^2 \phi - \sin^2 \phi_c)^2} \\ b^2 &= \frac{f^2 \sin^2 \phi}{\cos^2 \phi - \sin^2 \phi_c} \\ \frac{b^2}{a^2} &= \frac{|\cos^2 \phi - \sin^2 \phi_c|}{\cos^2 \phi} \end{aligned}\right\} \tag{36}$$

The conic is an ellipse, parabola or hyperbola as the discriminant

$$\Delta = (\cos^2\phi - \sin^2\phi_c) \gtreqless 0. \qquad (37)$$

As K/N is usually small ϕ will be close to ϕ_c, the $\Delta = 0$ value will appear when $\phi_c \doteq \pi/4$. This situation arises, as will be seen later, when one considers the formation of horizontal fringes in the 45° interferometer.

7. VERTICAL FRINGES

For vertical fringes $\bar{n}_4 \times \bar{n}_3$, the fringe direction, is perpendicular to the plane of centers of the interferometer. $\bar{n}_3$, $\bar{t}$ and consequently $\bar{p}$ all lie in the plane of centers. Since $\bar{p}$ is nearly perpendicular to the $\bar{x}$ direction of investigation, $\bar{p}$ will be almost parallel with $\bar{r}_c$ when $\bar{x} \cdot \bar{r}_c = 0$, i.e., when the normal to the photographic plate is $\bar{r}_c$. More precisely, $\bar{r}_c \cdot \bar{p} = 1$ implies

$$(\bar{r}_c \cdot \bar{n}_3) \cos(\psi - \epsilon/2) - (\bar{r}_c \cdot \bar{t}) \sin(\psi - \epsilon/2) = 1$$

or

$$\cos(\psi - \epsilon/2 - \theta) = 1 \qquad (38)$$

where θ is the angle of the interferometer. Equation (38) is satisfied if $\psi = \theta + \epsilon/2$, in other words, if the photographic plate is rotated through a positive angle $\theta + \epsilon/2$ from the $\bar{t}$ direction which lies along the trace of the mirror (3). The plate is thus seen to be parallel to the bisector of the angle between the $\bar{r}_{2c}$ and $-\bar{r}_{4c}$ vectors. This is the condition which E. H. Winkler has given for the plane of sharpest fringes. In this derivation it appears as the plane for which the largest source may be used to obtain fringes of a given clarity; for with $\bar{r}_c \cdot \bar{p} = 1$ the fundamental inequality becomes

$$1 - \frac{K}{N} \leq \bar{r} \cdot \bar{p} \leq 1 \leq 1 + \frac{K}{N} \; ; \qquad (39)$$

hence the admissible source is contained within the circle whose radius is

$$\rho = f \tan \phi_L \qquad (40)$$

where $\cos \phi_L = 1 - \frac{K}{N}$. Neglecting K^2/N^2 and higher powers, this relation becomes

$$\rho = f \sqrt{\frac{2K}{N}} \; , \qquad (41)$$

which is equivalent to Winkler's equation (2). It should be remarked that the argument given in deriving (41) is entirely independent of the angle of the interferometer and thus applies to

any in our general class. That (41) gives the largest permissible source is seen from the following heuristic argument: as $\bar{r}_c \cdot \bar{p}$ departs from value 1 the central cone is no longer degenerate. For small deviations, the excluded area near the center increases approximately as $f^2 \xi^2$ where ξ is the angle between $\bar{r}_c$ and $\bar{p}$. In the meantime, the outer area has remained practically constant; since, although the circle has become an ellipse of area πab, a and b are equal to within infinitesimals of the second order. The total available source area is seen to decrease. Aperture considerations restrict the usable source to the vicinity of the origin and so exclude the extreme case with $\xi \doteq \pi/4$ where the inner curve in the source plane is an ellipse while the outer curve is one branch of an hyperbola. Here the "interior" area is clearly infinite, but the usable region near the origin is extremely narrow and much less in area than that of the circle given above.

That (41) imposes a very weak restriction on source size may be seen by setting K = 1/10 and N = 200 fringes. For a 2" lens with f = 8", the diameter of the source is somewhat larger than half an inch. Practical spark sources used in high-speed interferometry have not approached this size to the author's knowledge.

8. HORIZONTAL FRINGES

It is possible to discuss the formation of fringes of any orientation by means of the analysis given above; however, we shall mention here only horizontal fringes. This case, which is representative of arbitrary orientations, is much more difficult to treat because the results depend strongly on the angle of the interferometer, e.g., whether it is a 45° or 30° interferometer has a strong effect on the permissible source.

As before, $\bar{n}_4 \times \bar{n}_3$ defines the fringe direction; and, as this is taken to be horizontal, it is clear that $\bar{n}_3$ and $\bar{n}_4$ and $\bar{t}$ all lie in the vertical plane. $\bar{n}_4$ may be rotated vertically out of the plane of centers through the angle $\epsilon/2$.

In order to obtain lengthwise clear fringes, it is necessary to orient the photographic plate to include the $\bar{n}_4 \times \bar{n}_3$ direction, i.e., it must be made to include the trace of mirror (3). Since $\bar{r}_c$ makes angle θ with $\bar{n}_3$ in the horizontal plane of centers and $\bar{p}$ must lie in a vertical plane containing $\bar{n}_3$, the smallest angle between $\bar{r}_c$ and $\bar{p}$ (consequently the largest source) is obtained when $\bar{n}_3 \cdot \bar{p} = 1$. Using (20), the expression for $\bar{p}$, as before we obtain

$$\cos(\psi - \epsilon/2) = 1 \qquad (42)$$

whence $\psi = \epsilon/2$ and the condition for clearest fringes (as given by E. H. Winckler) is to rotate the photographic plate around $\bar{n}_4 \times \bar{n}_3$ through $\epsilon/2$ from vertical. In this case, the plate is normal to $\bar{n}_4$.

Even in this favorable case $\cos\phi_c = \bar{r}_c \cdot \bar{p} = \cos\Theta$ and unless the interferometer chosen is one of extreme shear for which $\Theta \doteq 0$, the angle between $\bar{r}_c$ and $\bar{p}$ is appreciable.

In order to obtain an idea how the permissible source for a given interferometer appears, it is convenient to obtain approximate expressions for the constants of the conics neglecting terms in K^2/N^2 and higher. While the following equations are general, for horizontal fringes $\phi_c = \Theta$ will hold.

Since the limiting values of $\cos\phi$ are given by the fundamental inequality, we investigate only those curves for which

$$\cos^2\phi = (\cos\phi_c \pm K/N)^2 \quad , \tag{43}$$

where in this and the following expressions the upper sign refers to the upper limit, etc. The discriminant Δ in (37) becomes

$$\Delta \doteq \cos 2\phi_c \left(1 \pm g \frac{\cos\phi_c}{\cos 2\phi_c}\right) \gtrsim 0 \tag{44}$$

$$\text{with } g = \frac{2K}{N} .$$

We find for the center of the conic (35)

$$x \doteq \frac{f/2 \tan 2\phi_c}{1 \pm \frac{g \cos\phi_c}{\cos 2\phi_c}} \tag{45}$$

$$\doteq f/2 \tan 2\phi_c \left(1 \mp \frac{g \cos\phi_c}{\cos 2\phi_c}\right) \tag{46}$$

$$\text{when } \frac{g \cos\phi_c}{\cos 2\phi_c} \ll 1.$$

Similarly

$$a \doteq \pm f/2 \tan 2\phi_c \frac{\left(1 \mp \frac{g \cot 2\phi_c}{\sin\phi_c}\right)}{\left(1 \pm \frac{g \cos\phi_c}{\cos 2\phi_c}\right)} \quad , \tag{47}$$

$$\doteq \pm f/2 \tan 2\phi_c \left[1 \mp \frac{g\,(1 + \cos^2 2\phi_c)}{\sin\phi_c \sin 4\phi_c} \right] , \qquad (48)$$

$$b \doteq \pm \frac{f}{\sqrt{2}} \sqrt{\frac{1 - \cos 2\phi_c}{\cos 2\phi_c}} \frac{\left[1 \mp \frac{g \cos\phi_c}{2 \sin^2 \phi_c} \right]}{\left[1 \pm \frac{g \cos\phi_c}{2\cos 2\phi_c} \right]} \qquad (49)$$

$$\doteq \pm \frac{f}{\sqrt{2}} \sqrt{\frac{1 - \cos 2\phi_c}{\cos 2\phi_c}} \left[1 \mp \frac{g \cos^3 \phi_c}{2\sin^2 \phi_c \cos 2\phi_c} \right] \qquad (50)$$

and

$$\frac{b}{a} \doteq \frac{\sqrt{|\cos 2\phi_c|}}{\cos\phi_c} \frac{\left[1 \pm \frac{g \cos\phi_c}{\cos 2\phi_c} \right]^{\frac{1}{2}}}{\left[1 \pm \frac{g \cos\phi_c}{\cos^2 \phi_c} \right]^{\frac{1}{2}}} \qquad (51)$$

$$\frac{b}{a} \doteq \frac{\sqrt{|\cos 2\phi_c|}}{\cos\phi_c} \left[1 \pm \frac{g\,(1 - \cos 2\phi_c)}{4 \cos\phi_c \cos 2\phi_c} \right] . \qquad (52)$$

Using these equations and assuming $\Theta = \pi/4$, a 45° interferometer, we find that the permissible source of $K = 1/10$, $N = 200$ is the area contained between an ellipse and an hyperbola in the source plane. The constants of these figures are as follows:

Ellipse; $x \doteq 707f$

$a \doteq \pm 707f$

$b/a \doteq \frac{1}{\sqrt{707}} \doteq \frac{1}{27}$

Hyperbola; $x \doteq -707f$

$a \doteq \pm 707f$

with asymptotes $y \doteq \pm \frac{1}{\sqrt{707}}\, x$

The result is the extremely narrow, nearly horizontal, ribbon area imprisoned in the first and fourth quadrants between the conics given above. The origin is, of course, included in the source.

For the 30° interferometer, $\theta = \pi/6$, both conics are ellipses with the following constants:

$$x \doteq \sqrt{3}/2\ f(1 \mp \sqrt{3}\ g)$$

$$a \doteq \sqrt{3}/2\ f(1 + 5\sqrt{3}/3\ g)$$

$$b/a \doteq \sqrt{2/3}\ (1 \pm \sqrt{3}/6\ g)$$

from which it is clear that with $g = 10^{-3}$ as before, the ellipses are not far from circular as $b/a \doteq .816$. The width of the source on the axis is about .014f. This compares with the diameter $2\sqrt{g}\ f = .063f$ for the case of vertical fringes. Aperture limitations set by plate (4) or the camera lens are likely to restrict the useful source to less than 0.1 radian in angular width, in which case the circular source of .063 radians angular diameter will have a clear advantage in useful area.

The practical situation of interest with horizontal fringes is, of course, that for which the photographic plate is perpendicular to $\bar{r}_c$. Since this plane no longer contains the $\bar{n}_4 \times \bar{n}_3$ direction there will be a non-zero component of $\bar{x}_p$ in the plane normal to $\bar{n}_4 \times \bar{n}_3$ for all points except the origin. Investigating the boundaries of a circular field in the photographic plate is equivalent to exploring an ellipse in the plane perpendicular to $\bar{n}_4 \times \bar{n}_3$. The $\bar{p}$ vector will be nearly normal to the arbitrary vector on this ellipse.

For each $\bar{p}$ vector (i.e., for each $\bar{x}$ direction in the plane of the ellipse) the permissible source will lie between the two conics defined by the upper and lower bounds of the fundamental inequality. As there will be an infinity of different $\bar{p}$ vectors, there will be a corresponding infinity of pairs of conics. The permissible source is thus the common area between all pairs of conics in the infinite set. To determine this area is a complicated calculation which we shall not attempt here. Suffice it to say that the resulting source will be much more restricted than in any of the previous examples.

9. ACKNOWLEDGMENTS

The author wishes to express his thanks to Dr. J. H. Giese and Mr. D. B. Sleator for many helpful discussions of this work.

Frederick D. Bennett

Frederick D. Bennett

DISTRIBUTION

No. of Copies	
4	Chief of Ordnance Washington 25, D. C. Attn: ORDTB - Bal Sec
10	British - to ORDTB for distribution
4	Chief, Bureau of Ordnance Department of the Navy Washington 25, D. C. Attn: Re3
1	Commanding Officer Naval Proving Ground Dahlgren, Virginia
2	Office of Naval Research Department of the Navy Washington 25, D. C. Attn: Scientific Literature Branch (N482)
3	Commander Navy Ordnance Laboratory White Oak Silver Spring 19, Maryland
1	Commander Naval Ordnance Test Station Inyokern, California P. O. China Lake, California Attn: Technical Library and Editorial Section
1	Superintendent of Postgraduate School U. S. Naval Academy Annapolis, Maryland
1	Commanding Officer Naval Aviation Ordnance Test Station Chincoteague, Virginia

No. of Copies	
1	Commanding General Air University Maxwell Air Force Base Montgomery, Alabama Attn: Air University Library
4	Commanding General Air Materiel Command Wright-Patterson Air Force Base Dayton, Ohio Attn: Dr. T. Zobel
1	National Advisory Committee for Aeronautics Flight Propulsion Laboratory Cleveland, Ohio
2	National Advisory Committee for Aeronautics Ames Laboratory Moffett Field, California Attn: Mr. V. J. Stevens Mr. Harvey Allen
2	National Advisory Committee for Aeronautics Langley Field, Virginia
1	North American Aviation, Inc. Aerophysics Laboratory Los Angeles 45, California
1	United Aircraft Corporation Research Department East Hartford, Connecticut
1	Professor F. H. Clauser Department of Aeronautical Engineering The Johns Hopkins University Baltimore 18, Maryland

DISTRIBUTION

No. of Copies		No. of Copies	
2	California Institute of Tech. Jet Propulsion Laboratory Pasadena, California Attn: Prof. H. W. Liepmann Prof. H. T. Nagamatsu	1	Prof. D. Bershader University of Maryland College Park, Maryland
1	Prof. M. V. Morkovin University of Michigan Aeronautical Research Center Willow Run Airport Ypsilanti, Michigan	2	Applied Physics Laboratory The Johns Hopkins University 8621 Georgia Avenue Silver Spring, Maryland
1	Dr. A. E. Puckett Hughes Aircraft Company Florence Avenue at Teal Street Culver City, California	1	Prof. R. J. Stoner Physics Department Penn State College State College, Pennsylvania
1	Cornell Aeronautical Laboratory 4455 Genesee Street Buffalo 5, New York	1	Director National Bureau of Standards Connecticut Ave. at Van Ness St., N.W. Washington 25, D. C.
1	Prof. L. S. G. Kovaszny The Johns Hopkins University Baltimore 18, Maryland	1	Prof. Ernest Newmann Gas Turbine Laboratory Massachusetts Institute of Tech. Cambridge 39, Massachusetts
1	Prof. W. Bleakney Palmer Physical Laboratory Princeton University Princeton, New Jersey		
1	Prof. R. Ladenburg Palmer Physical Laboratory Princeton University Princeton, New Jersey		
1	Prof. H. W. Emmons Graduate School of Engineering Harvard University Cambridge 38, Massachusetts		
2	Prof. J. O. Hirschfelder Chemistry Department University of Wisconsin Madison, Wisconsin		


BALLISTIC